



1 Design of advanced airfoil for stall-regulated wind turbines

2 **Francesco Grasso¹, Domenico Coiro², Nadia Bizzarrini², Giuseppe Calise²**

3 ¹ Aerodynamix, Napoli, 80128, ITA – Contact Author: skyflash@inwind.it

4 ² Dip. Ingegneria Industriale, Università di Napoli FedericoII, Napoli, 80123, ITA

5 **Abstract.** Nowadays, all the modern MW-class wind turbines make use of pitch control to
6 optimize the rotor performance and control the turbine. However, for kW-range machines,
7 stall-regulated solutions are still attractive and largely used for their simplicity and robustness.
8 On the design phase, the aerodynamics plays a crucial role, especially concerning the
9 selection/design of the necessary airfoils. This is because the airfoil performance should
10 guarantee high wind turbine performance, but also the needed machine control capabilities. In
11 the present work, the design of a new airfoil dedicated for stall machines is discussed. The
12 design strategy makes use of numerical optimization scheme where a gradient-based algorithm
13 is coupled with XFOIL code and an original Bezier-curves-based parameterization to describe
14 the airfoil shape. The performances of the new airfoil are compared in free and fixed transition
15 conditions. In addition, the performance of the rotor is analysed comparing the impact of the
16 new geometry with alternative candidates. The results show that the new airfoil offers better
17 performance and control than existing candidates do.

18

19 1. Introduction

20 Looking back in wind turbines history, pitch-regulated machines gradually substituted stall-regulated
21 systems. In fact, the possibility to optimize the power production for each wind condition by
22 regulating the pitch angle of the blade, proved to be a key feature to maximize the Annual Energy
23 Production (AEP) of the wind turbines. Nowadays, all the modern MW-class wind turbines are “by
24 default” pitch-regulated and several innovations are implemented by Industry to improve the pitch
25 performance (e.g. individual pitch control, fine regulation mechanisms/algorithms) and extract more
26 power.

27 In apparent contradiction with MW machines however, small and medium kW wind turbines are
28 still largely stall-regulated machines. The reasons of this are easy to explain. In fact, the advantages of
29 the pitch system come with some costs. The first is the direct cost of the pitch system and its
30 maintenance. Secondly, the pitch system increases the general complexity of the system, together with
31 the development costs and the issues related to the system robustness/reliability. Extra components,
32 such onboard anemometers, pitch bearings are necessary to operate correctly the pitch of the blade. All
33 these costs and complications can be very relevant for small machines and it explains why a robust
34 and easy-to-maintain solution is preferred even with some AEP sacrifice.

35 From the design point of view, the stall-regulated machines offer still a challenging task, especially
36 concerning the aerodynamics of the blade that should ensure the power performance but provide the
37 machine control. In practice, the design of the blade should obviously aim to maximize the AEP, but it
38 is also the only component to keep the turbine under control and stopping it when necessary. To do so,
39 the stall and post-stall characteristics of the airfoils play a crucial role. From this angle, the



40 selection/design of the airfoils and the blade shape design are more delicate than pitch-regulated
41 turbines.

42 The present work focuses on the design of a new airfoil specifically designed for stall-regulated
43 turbines. The next section illustrates the design of the new airfoil in comparison with existing
44 geometries. Then, its impact on the overall turbine performance is discussed.

45 **2. Design of the new airfoil**

46 *2.1. General requirements*

47 The selection of the proper airfoils is very relevant to achieve satisfactory wind turbine performance.
48 Depending on the area of the blade, the requirements change quite a lot; in fact, the outer sections are
49 optimized for high aerodynamic performance, while the inner sections are designed to provide low-
50 weight, structural integrity to the blade.

51 The focus of the present investigation is the outer region of the blade, so the airfoils should have high
52 aerodynamic efficiency (L/D). This is the primary parameter to increase the annual energy production
53 of the rotor, but it is not the only one. Besides that, the stall behaviour should be considered, avoiding
54 sharp stall. This would lead in fact to load problems to the blade (e.g. fatigue issues and additional
55 noise) and other components. The impact of roughness on the rotor performance should be also
56 addressed when the airfoil is designed/selected. Normally, the annual production decreases when the
57 blade is contaminated by dirtiness (e.g. mosquitos), damages (e.g. erosion) or imperfections.
58 Designing an airfoil that is robust (or less sensitive) to roughness would contribute to maintain a stable
59 performance on the long run. Thus, it is important to have airfoils with reduced drop in maximum lift
60 coefficient and aerodynamic efficiency in rough conditions. In addition, limited variations in terms of
61 corresponding angles of attack are desirable.

62 Looking at the blade construction, it must be buildable and lightweight to save the production costs,
63 so the airfoils adopted should not have critical features which may compromise those aspects (e.g. too
64 thin trailing edge, very concave-complex areas). Inevitably, there is interaction between weight
65 minimization and annual energy production optimization, where the first would drive for instance, to
66 large thickness distribution to accommodate a structurally efficient spar and maximize the section's
67 moment of inertia, while the second would tend to reduce the airfoil thickness to reduce the drag.

68 A complete discussion can be found in Grasso, 2011.

69 *2.2. Aerofoils for stall-regulated wind turbines*

70 In addition to what presented in the previous paragraph, special considerations should address the
71 peculiarity of stall-regulated wind turbines. As mentioned, the big challenge of these machines is their
72 control. While the pitch-regulated turbines can change the pitch angle of the blades, so to optimize the
73 performance for each wind speed, the stall-regulated turbines are much simpler and rely only on the
74 aerodynamics of the airfoils. This increases the complexity of the airfoil design

75 First of all, the airfoils of stall regulated turbines work in a quite wide range of angles of attack so a
76 sound performance comes from the fact that they achieve high aerodynamic efficiency over the angle
77 of attack range. This is an important element to properly setup the design process. In fact, a design
78 point close to stall would be desirable to obtain best AEP performance and the margin must be
79 carefully calibrated and reduced compared to the values for pitch-regulated machines. The stall
80 mechanism stops the turbine when the loads are becoming too large; postponing the stall could lead to
81 excessive forces on the blades and the other components of the turbine. Furthermore, the capability to
82 control the machine, slowing down the rotor and avoiding over-power issues depends on the airfoil
83 stall and post-stall behaviour. In fact, a slope of the lift curve excessively “flat” could be insufficient to
84 control the turbine (and so prevent over-power), while sharp stall would make more difficult to re-start
85 the machine and would cause sudden changes into the loads faced by the blades. In addition to this, the
86 airfoil post-stall response is fundamental to avoid stall-induced vibrations, which is one of the main
87 issues to address in designing stall-regulated machines.



88

89 *2.3. The stall-induced vibration phenomena and its impact on airfoil design*

90 When a wind turbine blade vibrates, the aerodynamic forces have an additional component originated
91 by the vibration velocity. Such component with good approximation can be considered proportional to
92 vibration velocity, thus it actually acts as a viscous damping force, usually denoted as “aerodynamic
93 damping” (see Petersen et al., 1998, Rasmussen et al., 1993, Rasmussen, 1994. When the airfoils are
94 in stall conditions, the slope of the lift curve becomes negative and can cause a local negative
95 aerodynamic damping in the lift direction.

96 As in instance, a descending airfoil will see an increasing angle of attack that will cause a lower value
97 of lift coefficient; this will be equivalent to have a component of the aerodynamic force promoting the
98 descent of the airfoil, thus acting as a negative damping force.

99 If global aerodynamic damping of the blade is both negative and larger (in magnitude) than the
100 structural damping, any disturbance can cause divergent oscillations which can dramatically increase
101 fatigue loads and can even lead to rapid failure in the worst case.

102 This phenomenon is usually reported as “stall induced vibrations” and represents a key issue for stall
103 regulated wind turbines, which work in stalled conditions for a significant part of the lifetime.

104 Stall induced vibrations have to be intended as instabilities of the blades that can take place due to any
105 initial disturbance. A sharp stall leads to lower damping force and so larger vibrations. On the other
106 hand, a flat lift curve beyond the stall could be insufficient to control the turbine.

107 Low stall induced vibrations and power control represent two conflicting requirements which make
108 the design of a stall regulated wind turbine a highly complex challenge. Finding a good compromise
109 between these two aspects has been one of the main efforts in this work.

110 During the preliminary design phase, a simplified expression of the aerodynamic damping of the blade
111 has been used (implemented) to predict the dynamic behaviour of the blades without the need of any
112 aeroelastic analysis, to make the design as fast as possible.

113 The linearized approach presented by Petersen et al., 1998 has been applied to obtain a simplified
114 expression for the local aerodynamic damping on the different sections of the blades, only using quasi-
115 steady, 2-D aerodynamics of the airfoils. Then, a simplified modal approach has been implemented to
116 evaluate the aerodynamic damping of the complete blade, obtaining a damping coefficient (DC) used
117 as an index of eventual oscillations amplitude. The use of this damping coefficient has been validated
118 with several cases of wind turbines obtained during the optimization process, giving always results
119 coherent with the behaviour of the blades evaluated through aeroelastic analysis.

120 From the expression of the local damping coefficient in the out-of-plane direction (that usually is very
121 close to the flap-wise direction), it is possible to notice that a gentle stall of the airfoils along the blade

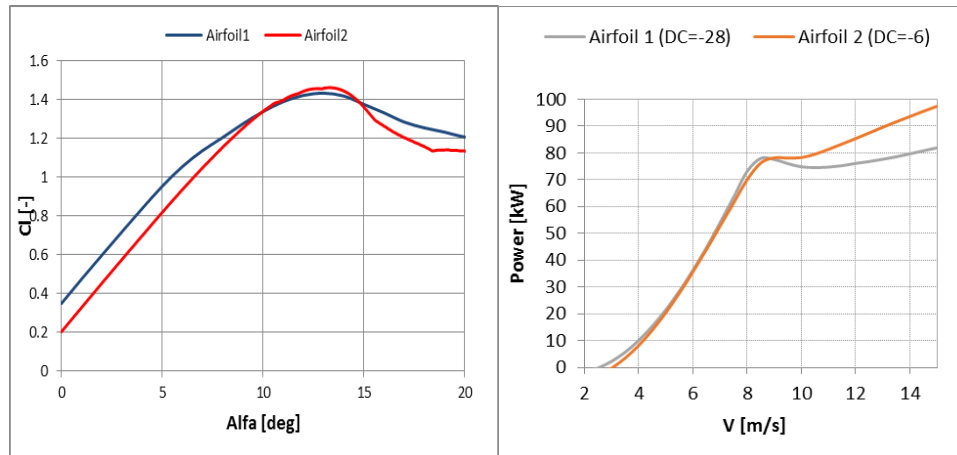
122 (which means a small value of the absolute value $|\frac{dcl}{d\alpha}|$ beyond the stall) would be desirable to avoid

123 the occurrence of stall induced vibrations. The expression of modal damping coefficients (both in
124 edge-wise and in flap-wise directions) provides another useful information for the optimization
125 process. For each direction and for each mode, the modal aerodynamic damping coefficient can be
126 interpreted as a linear combination of the local damping coefficients of the different sections along the
127 blade, each one multiplied by the local displacement related to the mode shape. Looking at typical
128 modes shapes of a wind turbine blade, considered as a cantilevered beam, it can be observed that the
129 highest displacements always occur on the outer part of the blade. This means that the largest
130 contribution to the damping of the blade is given by the outer sections. Thus, the blade optimization to
131 avoid stall-induced vibrations can be limited at this part of the blade.

132 Typical effect of using in the outer half of the blade an airfoil with a smoother stall is shown in the
133 following figure, in terms of power curve and modal aerodynamic damping coefficient (DC). It can be
134 noticed how a gentle slope of lift coefficient curve of the airfoils (Airfoil 1) results in a reduction of
135 the absolute value of DC with the related stall induced vibrations but in a less power control at high
136 wind speeds. The loss of power control is due to higher lift coefficients in the post-stall regime, caused
137 by the smoother stall of the airfoil.



138



139
140

Figure 1 Power curve generated (right side) as effect of different airfoil stall behavior (left side).

141

142 So overall, it is important that the stall margin is reduced but with gentle and continuous stall. To limit
143 the problem of power control the airfoils along the blade should have a low lift coefficient beyond stall
144 and the drag coefficient as high as possible.

145 To complete the challenging scenario, these characteristics must be achieved both in clean and rough
146 conditions. This introduce more complexity for the designer because special attention should be put
147 also to avoid that the characteristics of the lift curve do not change significantly to influence the stall
148 and post-stall behaviour.

149 During the rotor design, the ‘rough’ power curve is considered because it is the most conservative in
150 terms of overall performances and power control. The ‘clean’ power curve is considered because it is
151 the most conservative for extreme and fatigue loads (due to higher stall induced vibrations due to a
152 more abrupt stall).

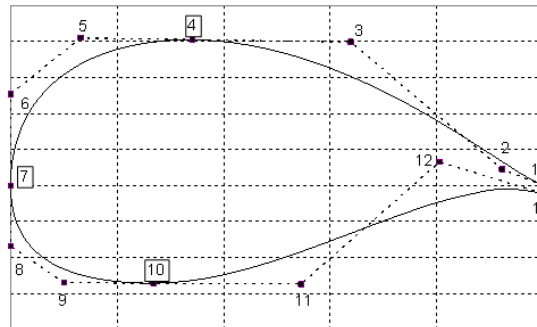
153 2.4. Design methodology

154 Multidisciplinary Design Optimization (MDO) (see Fletcher, 1987) has been adopted in this work. In
155 fact, when compared to a traditional design technique (e.g. inverse design), MDO leads to a more
156 accurate and computational-time saving design product, while covering constraints coming from
157 different disciplines. Based on author’s previous experience (see Bizzarrini et al. 2011, Grasso, 2012),
158 a gradient-based algorithm (Zhou et al., 1999) has been preferred to control the design procedure,
159 where the popular tool RFOIL (van Rooij, 1996) is used to evaluate the aerodynamic performance of
160 the airfoil. In fact, RFOIL accuracy for stall region is significantly better than XFOIL (Drela, 1989)
161 and, as mentioned in the previous chapters, stall is quite crucial parameter in this case.

162 The geometry of the airfoil is parameterized with a combination of four Bezier curves (see Prautzsch
163 et al., 2002, Barsky, 1990, Beach, 1991) of third order distributed along the airfoil contour (figure 2).
164 Each Bezier curve covers one quarter of the shape with 13 control points free to move in chord and
165 normal-to-the-chord directions (i.e. 26 design variables). To appreciate and understand the choice of
166 four Bezier curves, the reader should consider that third order polynomial is needed to describe
167 inflection points; however higher degree can lead to wavy shapes. Dividing the airfoil contour in four
168 pieces is a smart move to divide the complexity of the parametrization and ease the control of the
169 shape. This formulation is C2 continuous. 15 design variables are active in the present work; in fact,
170 the leading edge cannot move, while the neighbours and the trailing edge can move only in vertical



171 direction. In addition, the control points 4 and 10 are internally controlled to ensure C2 property also
172 in those points. The complete mathematical formulation can be found in Grasso, 2008.
173



174
175 *Figure 2 Airfoil shape parameterization scheme. From Grasso, 2008.*

176 3. Results

177 3.1. Airfoil performance

178 The blade in development has two airfoils only (one main and one at the inner part, excluding the
179 blending area at the very root of the rotor) in order to simplify the blade construction. This work
180 focuses on the main airfoil design where the main target is the aerodynamic efficiency (L/D)
181 maximization at the operative Re number of 1 million. At the same time, appropriate stall behaviour
182 needs to be achieved in order to provide good control to the wind turbine. As already mentioned, this
183 aspect plays a crucial role in the present work. To cover this aspect, several options in terms of
184 constraints to be implemented have been considered. As high lift performance may lead to sharp stall
185 behaviour, a constraint limiting the maximum lift coefficient can be quite natural choice. However, it
186 may not be sufficient to limit the lift coefficient at a specific angle of attack, since there will be no
187 control on different angles. In fact, it could happen that the stall angle could delay or anticipate despite
188 the fact that the constraint is satisfied. The same constraint could be assigned on several angles of
189 attack around the expected stall angle range, but this will gain little more confidence while adding
190 complexity to the optimization problem. This in general, would increase the risk of limiting too much
191 the design space and drive the solution to local optima. On top of that, there will be no guarantee on
192 post-stall characteristics which would require specific constraints. A better and more accurate
193 approach could be to evaluate the full polar at each design evaluation and retrieve the information
194 about maximum lift coefficient and post-stall, via the lift slope value. In this way, the number of
195 constraints will reduce to just two which would fully describe the stall behaviour, keeping low the
196 mathematical complexity of the optimization problem. However, the computational time would rise
197 because the full polar needs to be calculated for any iteration. On top of that, the same approach
198 should be used in rough conditions to make sure that the airfoil has same characteristics in both cases.
199 Although the latest approach would be the most accurate, a different approach has been adopted in the
200 present work, which should be more practical but still with some good accuracy level. A combination
201 of constraints focused on maximum lift coefficient (<1.4) and moment coefficient (>-0.12) has been
202 prescribed. In fact both constraints act on the shape of the lift curve bounding its maximum point and
203 its average position in lift axis (i.e. defining the α zero lift or the lift at zero degrees), respectively.
204 Considering the airfoil geometry, both constraints have a direct impact on the camber line of the airfoil
205 and their combined effect is to get soft stall with no excessive cambered shape. Since the roughness
206 generally has little influence on the linear region of the moment coefficient curve, the same constraint
207 on clean conditions should cover also the rough condition.



208 The airfoil thickness (t/c) of 0.25 has been selected, rather than a thinner value. Although the pure
209 aerodynamic performance could be better with thinner (e.g. t/c 0.15, 0.18) airfoils, thicker sections
210 offer the advantages of saving blade mass and provide higher strength to the blade structure.
211 Considering existing airfoils, the S821 and the S819 have been used as reference (Somers, 1993,
212 Tangler et al., 1995, Somers, 1998). Figure 3 shows the shapes, while figures 4 – 6 show the
213 aerodynamic performance of these airfoils in free and fixed transition, as calculated with the RFOIL
214 code. The Reynolds number used for the simulations is 1 million, in accordance with the average real
215 Reynolds number value expected for a 60kW-range machine. It should be noticed the stall and post-
216 stall behaviour that is soft but monotonically decreasing in the indicated angle of attack range. In
217 addition, it should be noticed the relative small margin between the design point and the stall; for stall-
218 regulated turbines, this is an important feature to avoid excessive loads once the design condition has
219 been passed (e.g. in case of wind gust).
220

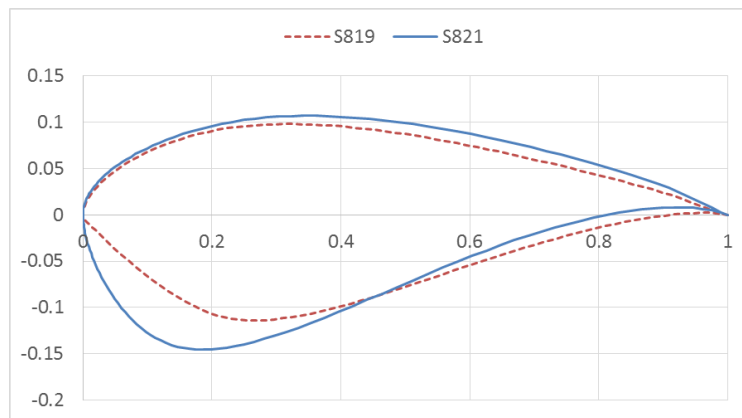


Figure 3 S819 and S821 shapes.

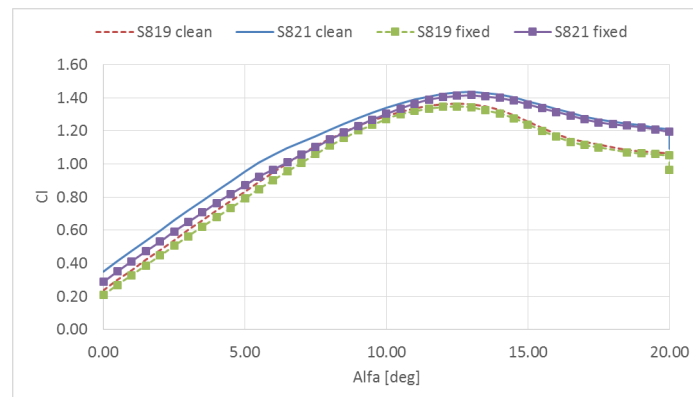
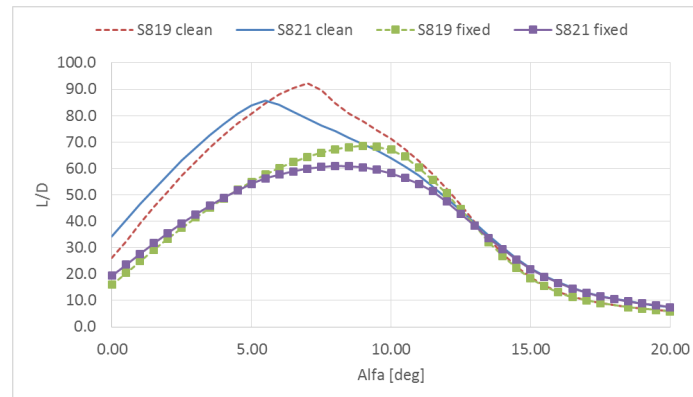


Figure 4 Lift curves for S819 and S821 airfoils. Free and fixed transition data, 1 million Re number. RFOIL predictions.

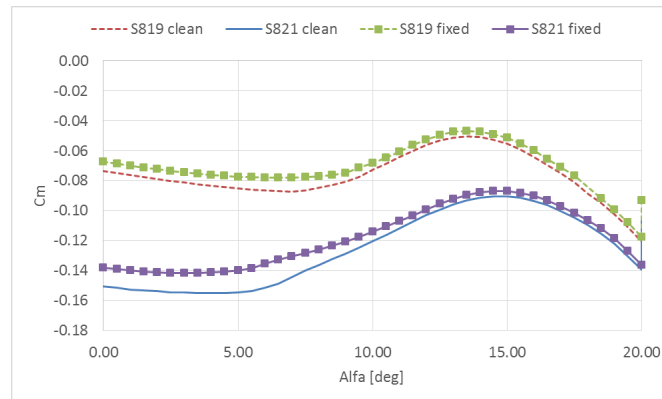
221
222

223
224



225
226
227

Figure 5 Aerodynamic efficiency curves for S819 and S821 airfoils. Free and fixed transition data, 1 million Re number. RFOIL predictions.



228
229
230

Figure 6 Moment coefficient for S819 and S821 airfoils. Free and fixed transition data, 1 million Re number. RFOIL predictions.

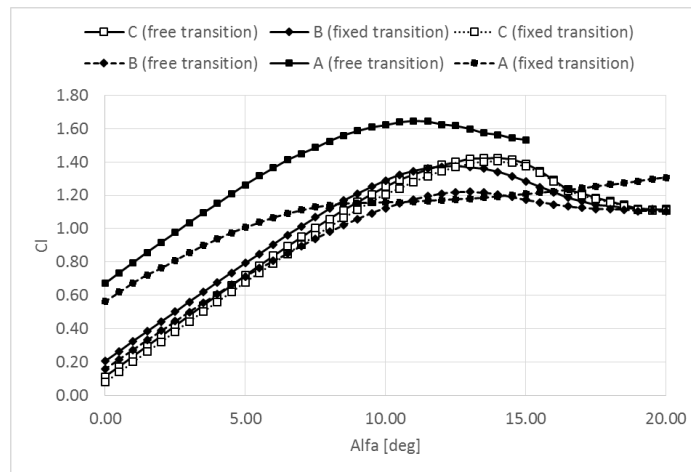
231 So the ideal airfoil is a 25% thick shape (similar to the S821 which is 24% thick) with L/D
232 performance similar to S819, reduced stall margin and maximum lift coefficient (C_{lmax}), but also
233 small roughness sensitivity and contained moment coefficient (C_m); the latter to avoid excessive
234 torsional loads.

235 With these parameters in mind, three airfoils have been developed to offer better performance than the
236 reference geometries. The airfoils have been preliminary named A, B and C and are all 25% thick (the
237 shapes are not shown because of confidentiality issues). Their aerodynamic characteristics, evaluated
238 with RFOIL, are illustrated in figure 7 and 8.

239 The airfoil A has more camber than the other airfoils since the constraint on moment coefficient
240 discussed above has not been used in order to check the validity of the assumption. This is evident
241 from the lift curve. It achieves better efficiency in clean condition. However, its behaviour is very
242 sensitive to the roughness; in fixed transition, the efficiency drops significantly and the lift curve
243 changes completely, making impossible the control of the wind turbine. The differences are smaller
244 for the airfoil B, but the post-stall characteristics of the lift curve make difficult the control of the
245 turbine. The airfoil C (from now on, called G25sx6) is instead a good compromise between good
246 performance and good control properties. The lift curve is in practice almost unchanged from free to
247 fixed transition, as result of adopting the constraint on moment coefficient and lift coefficient. In

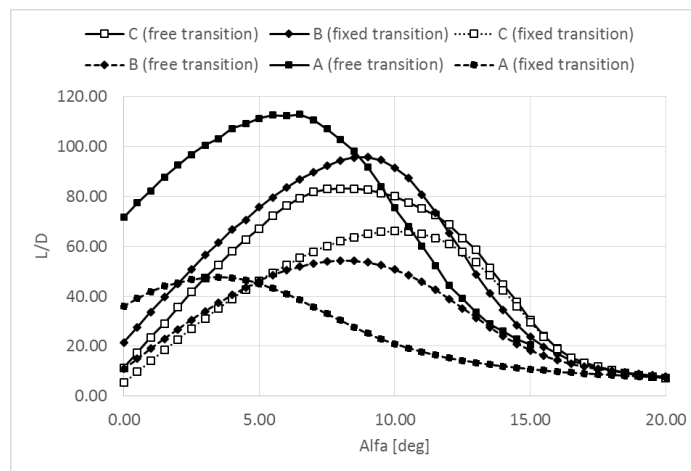


248 addition, the stall angle of attack is unchanged. In terms of efficiency, the G25sx6 exhibits the best
 249 performance in fixed transition and a quite flat plateau in both free and fixed transition. As mentioned,
 250 this is quite convenient for stall regulated turbines because the airfoil will operate in a range of angles
 251 of attack rather than a specific value like in the pitch controlled machines. Combining lift and
 252 efficiency performance, the stall margin is almost unchanged between free and fixed transition.
 253



254
 255

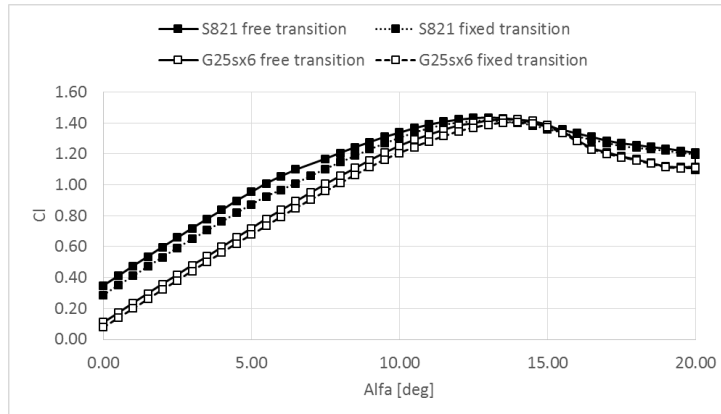
Figure 7 Lift curve of the new airfoils. Free and fixed transition data, 1 million Re number. RFOIL predictions.



256
 257
 258

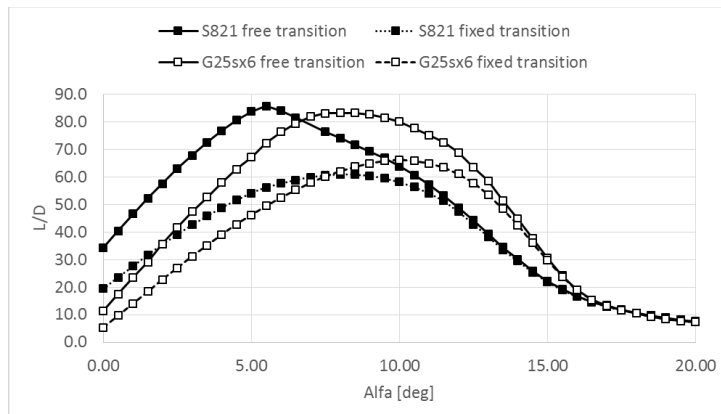
Figure 8 Aerodynamic efficiency curve of the new airfoils. Free and fixed transition data, 1 million Re number. RFOIL predictions.

259 Comparing the G25sx6 with the S821 airfoil (figures 9 and 10) it can be noticed a similar value of
 260 efficiency in free transition but better performance in fixed transition despite the G25sx6 is thicker
 261 (25%) than the S821 (24%).
 262 In addition, the efficiency curves keep a good level over a wider range of angles of attack and the stall
 263 margin is reduced, that is an advantage for stall regulated wind turbines (i.e. avoiding excessive loads
 264 in case of wind gust).
 265



266
 267

Figure 9 Lift curve of the new airfoil. Free and fixed transition data, 1 million Re number. RFOIL predictions.

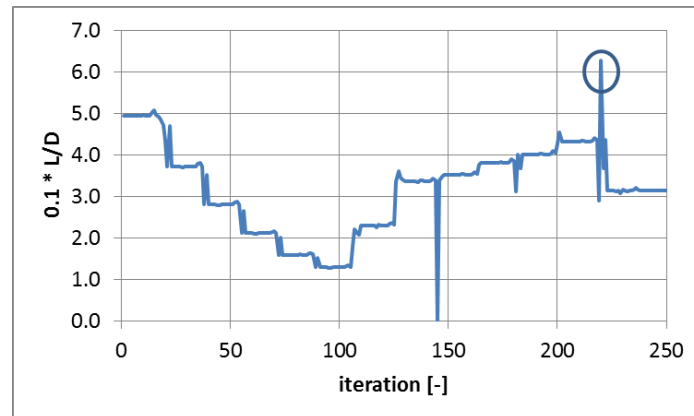


268
 269
 270

Figure 10 Aerodynamic efficiency curve of the new airfoil. Free and fixed transition data, 1 million Re number. RFOIL predictions.

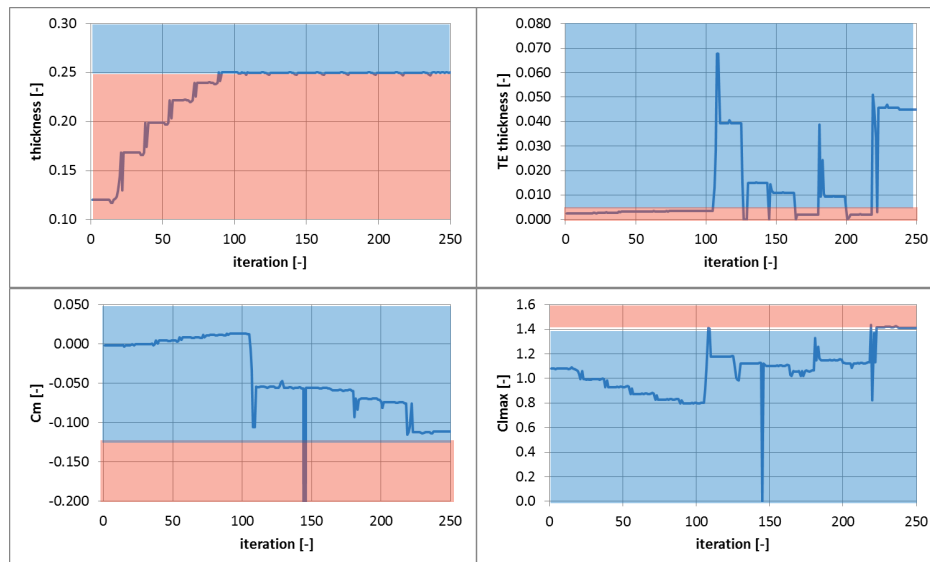
271 **3.2. Optimization process details**

272 This section presents some of the details of the optimization process for the G25sx6 airfoil. As
 273 mentioned in the previous paragraph, the L/D was used as parameter to be maximized. To obtain good
 274 roughness robustness, the design has been performed in fixed transition conditions; in addition, the
 275 L/D value was divided by a factor 10 to have the same order of magnitude ($o1$) used for the
 276 constraints. Figure 11 shows the evolution of the objective function during the iterations of the
 277 optimization process. As it can be observed, the trend is not monotonically increasing as one could
 278 expect. This is because, to reduce the risk to obtain a local optimal solution, the NACA0012 airfoil has
 279 been used as initial solution, which is out of the feasible domain (t/c violating the threshold value) and
 280 so far from any possible feasible local optima. The optimization algorithm is designed to obtain first a
 281 feasible solution (if any) and then optimize it inside the domain space. Roughly the first 100 iterations
 282 are used to obtain a feasible solution. This is evident by looking at figure 12 where the evolution of the
 283 constraints is illustrated, together with their threshold values identified by the division between the
 284 feasible domain (blue area) and the unfeasible one (red area). The circle in figure 11 corresponds to
 285 the optimal solution.
 286



287
 288

Figure 11 Evolution of the objective function during the design process. Optimal solution highlighted in the circle.



289

290
 291
 292

Figure 12 Evolution of the constraints during the design process. The blue region corresponds to the feasible domain, while the red one corresponds to the infeasible domain.

293 3.3. Impact on rotor performance

294 In order to assess the value of the new airfoil, its impact on wind turbine performance has been
 295 evaluated with a numerical analysis.

296 A 60kW stall-regulated wind turbine has been used as reference and the S821 and G25sx6 airfoils
 297 have been adopted as main airfoil. The reference wind turbine is a three blades machine designed to
 298 product energy in sites characterized by a very low mean wind speed, such as coastal regions but also
 299 many hinterland areas. Thus, its main characteristics are very low values of cut-in and power peak
 300 wind speeds (about 2.5 m/s and 8.5 m/s respectively) and a high AEP with a mean wind speed of
 301 about 4 m/s. To obtain this performance a generous rotor radius and particularly slender blades are
 302 adopted: the radius is 14 m and the rotational speed is constant 34 rpm.



303 Figure 13 shows the power curves for the blade optimized based on the S821 airfoil and G25sx6
304 airfoil. The BEM-based (Hansen, 2007) tool WtPerf (Buhl, 2004) developed by the NREL has been
305 used for these analyses.
306 The blade geometry has been adjusted to consider the actual airfoils adopted. Normally, this includes
307 chord and twist; however in this case, the same chord distribution has been used (figure 13) since
308 preliminary analyses showed little impact on overall performance.
309

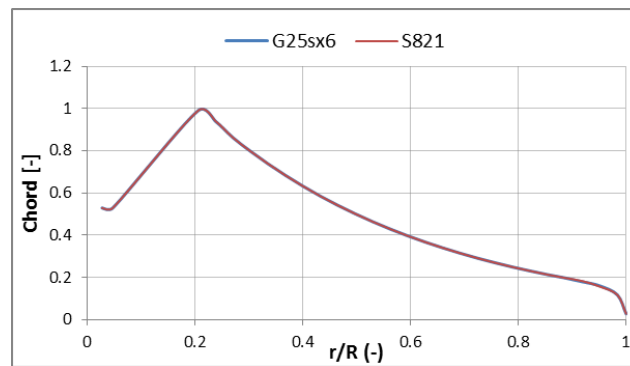


Figure 13 Chord distribution adopted during the blade design.

310
311

312 As already mentioned, the G25sx6 is 1% thicker than the S821; this ensures a higher moment of
313 inertia of each section implying a lower weight of the blade. From a preliminary analysis, the weight
314 of the blade can be reduced of about 5%.
315 Both free and fixed transition conditions have been included, as representative of clean and rough
316 blade conditions. The power curves related to free and fixed transition in the figure refer to different
317 values of the blade pitch, which is the value necessary to achieve the desired power peak in each case.
318 Since in fixed transition the lift coefficient (particularly the maximum lift coefficient) is lower than in
319 free transition, a larger value of pitch angle will be necessary to reach the desired power peak. At the
320 same time, higher wind speed is needed to reach the same power peak.
321

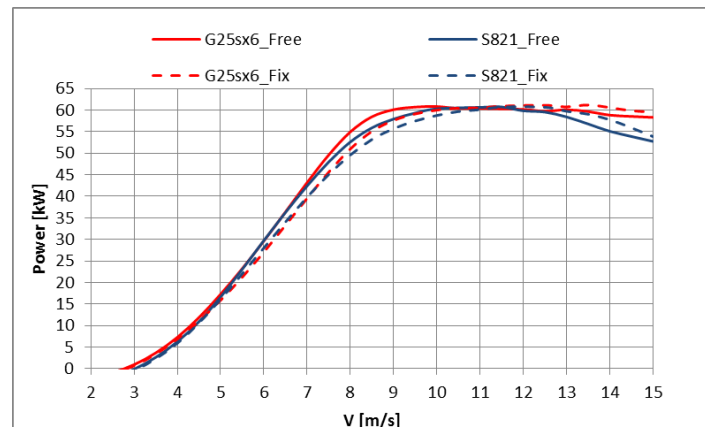


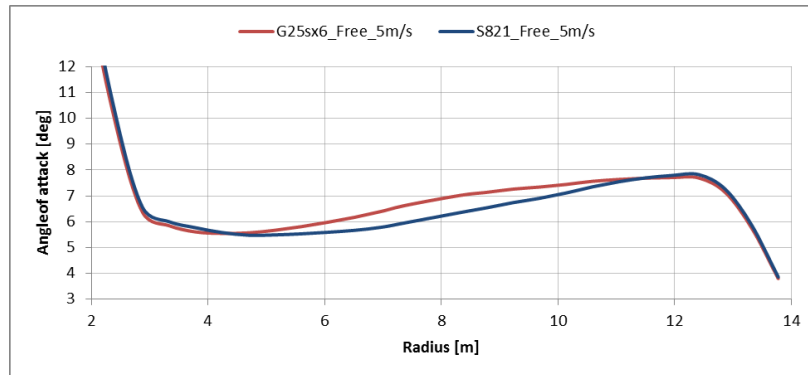
Figure 14 Effect of the new airfoil on the wind turbine power curve.

322
323

324 The following figure shows the angle of attack distribution along the blade at 5 m/s and in free
325 transition condition for both the wind turbines. The unusual distribution that can be noticed at the tip



326 of the blade is due to the twist distribution adopted to reduce stall-induced vibrations, reduce the loads
 327 and improve the overall stability; this feature, together with the rest of the blade design strategy and
 328 process will be discussed in a dedicated work.
 329



330
 331

Figure 15 Angle of attack distribution along the blade.

332

Table 1 Impact of the new airfoil on the wind turbine AEP.

Airfoil	Free transition		Fixed transition	
	AEP [kWh]	Δ [%]	AEP [kWh]	Δ [%]
S821	136000	-	129000	-
G25sx6	143000	+5.15	132000	+2.3

333

334 Considering the overall Annual Energy Production (AEP, see table 1), the new airfoil provides a
 335 considerable gain in free (+5.1%) and fixed (+2.3%) conditions. More in detail, the turbine reaches the
 336 maximum power for lower wind speed and the post-peak region is smoother. In addition, the
 337 production at very low wind speed increases thanks to the new airfoils.

338 4. Conclusions

339 Despite the pitch controlled wind turbines cover the complete large MW machines market, stall
 340 regulated solutions are still diffused for small power production. A new airfoil specifically designed
 341 for this class of wind turbines has been developed and presented in this work. Compared to existing
 342 geometries, the new airfoil can increase visibly the annual energy production of the machine, both in
 343 clean and rough conditions. In terms of rotor performance, the new airfoil brings a visible benefit on
 344 the punctual power production and on the overall AEP (+5.1% in free transition and +2.3% in fixed
 345 transition).

346 References

- 347 [1] Grasso, F., "Usage of Numerical Optimization in Wind Turbine Airfoil Design", AIAA, Journal of Aircraft,
 348 AIAA, Vol.48, No.1, Jan.-Feb. 2011, DOI: 10.2514/1.C031089.
 349 [2] Petersen, J.P., Madsen, H.A., Bjork, A., Enevoldsen, P., Oye, S., Ganander, H., Winkelaar, D., "Predictions of
 350 Dynamic Loads and Induced Vibration in Stall", Risoe, Risoe-R-1045, May, 1998.
 351 [3] Rasmussen, F., Petersen, J.T., Winkelaar, D., Rawlinson-Smith, R., "Response of Stall Regulated Wind
 352 Turbines – Stall Induced Vibrations", final report for Joule I Project, Contract no. JOUR-0076, DG XII, Report
 353 Riso-R-691 (EN), Risoe, June 1993.
 354 [4] Rasmussen, F., "Dynamic stall of a Wind Turbine Blade Section", Proceedings of the 8th IEA Joint Action
 355 Symposium on Aerodynamics of Wind Turbines, November 1994.
 356 [5] Fletcher, R., "Practical Methods of Optimization", Wiley, 1987, ISBN: 978-0471494638
 357 [6] Bizzarrini, N., Grasso, F., Coiro, D.P., "Genetic Algorithms in Wind Turbine Airfoil Design",
 358 Proceedings of EWEA2011, Bruxelles, March 2011.

359



- 359
360
361
362
363
364
365
366
367
368
369
370
371
372
373
374
375
376
377
378
379
380
381
382
383
384
385
386
387
- [7] Grasso, F., “Hybrid Optimization of Wind Turbine Thick Airfoils”, Proceedings from 9th AIAA Multidisciplinary Design Optimization Specialists Conference, Honolulu, 2012. AIAA 2012-1354, doi:10.2514/6.2012-1354
 - [8] Zhou, J.L., Tits, A.L., Lawrence, C.T., “User’s guide for FFSQP version 3.7: A FORTRAN code for solving constrained nonlinear optimization problems, generating iterates satisfying all inequality and linear constraints”, University of Maryland, College Park. 1999.
 - [9] van Rooij, R.P.J.O.M., “Modification of the boundary layer calculation in RFOIL for improved airfoil stall prediction”, Report IW-96087R TU-Delft, the Netherlands, September 1996.
 - [10] Drela, M., “XFOIL: An Analysis and Design System for Low Reynolds Number Airfoils, Conference on Low Reynolds Number Airfoil Aerodynamics”, Vol. 54 Lecture Notes in Engineering, University of Notre Dame, 5-7 June 1989. DOI: 10.1007/978-3-642-84010-4
 - [11] Prautzsch, H., Boehm, W., Paluszny, M., “Bezier and B-Spline Techniques”, Springer, 2002. ISBN: 978-3540437611.
 - [12] Barsky, B.A., “Acm/siggraph ’90 course 25: Parametric bernstein/bezier curves and tensor product surfaces”, Dallas, TX. Aug. 7th 1990.
 - [13] Beach, B.C., “An Introduction to Curves and Surfaces of Computer-Aided Design”, Van Nostrand Reinhold, 1991.
 - [14] Grasso, F., “Multi-Objective Numerical Optimization Applied to Aircraft Design”, Ph.D. Thesis, Dip. Ingegneria Aerospaziale, Università di Napoli Federico II, Napoli, Italy, December 2008.
 - [15] Somers, D.M., “The S819, S820 and S821 Airfoils”, NREL, NREL/SR-500-36334, October 1992-November 1993.
 - [16] Tangler, J. L.; and Somers, D. M.: NREL Airfoil Families for HAWTs. NREL/TP-442-7109, Jan. 1995.
 - [17] Somers, Dan M.: Effects of Airfoil Thickness and Maximum Lift Coefficient on Roughness Sensitivity. Airfoils, Inc., 1998.
 - [18] Hansen, M.O., “ Aerodynamics of wind Turbines, 2nd edition“, Routledge, December 2007. ISBN: 978-1844074389.
 - [19] Buhl, M. L., “WT_perf user’s guide”, National Wind Technology Centre, NREL, Golden, Co, USA, 2004.
 - [20] Abbott, I.H., Von Doenhoff, A.E., Theory of wing sections, including a summary of airfoil data, Dover Publications Inc., Dover edition. 1959.